

## DISCOVERY OF A GIANT STELLAR TIDAL STREAM AROUND THE DISK GALAXY NGC 4013

DAVID MARTÍNEZ-DELGADO<sup>1,2,8</sup>, MICHAEL POHLEN<sup>3,4</sup>, R. JAY GABANY<sup>5</sup>, STEVEN R. MAJEWSKI<sup>6</sup>, JORGE PEÑARRUBIA<sup>7</sup>,  
AND CHRIS PALMA<sup>6,9,10</sup>

<sup>1</sup> Instituto de Astrofísica de Canarias, La Laguna, Spain

<sup>2</sup> Max-Planck Institut für Astronomie, Heidelberg, Germany

<sup>3</sup> School of Physics & Astronomy, Cardiff University, Cardiff, UK

<sup>4</sup> Kapteyn Instituut, Rijksuniversiteit Groningen, Groningen, The Netherlands

<sup>5</sup> BlackBird Observatory, Mayhill, NM, USA

<sup>6</sup> Department of Astronomy, University of Virginia, Charlottesville, VA 22904-4325, USA

<sup>7</sup> Department of Physics & Astronomy, University of Victoria, Canada

Received 2008 January 25; accepted 2008 October 20; published 2009 February 23

### ABSTRACT

We report the discovery of a giant, looplike stellar structure around the edge-on spiral galaxy NGC 4013. This arcing feature extends 6′ (~26 kpc in projected distance) northeast from the center and 3′ (≈12 kpc) from the disk plane; likely related features are also apparent on the southwest side of the disk, extending to 4′ (~17 kpc). The detection of this low surface brightness ( $\mu_R = 27.0_{-0.2}^{+0.3}$  mag arcsec<sup>-2</sup>) structure is independently confirmed in three separate datasets from three different telescopes. Although its true three-dimensional geometry is unknown, the sky-projected morphology of this structure displays a match with the theoretical predictions for the edge-on, projected view of a stellar tidal stream of a dwarf satellite moving in a low inclined (≈25°), nearly circular orbit. Using the recent model of the Monoceros tidal stream in the Milky Way by Peñarrubia and colleagues as a template, we find that the progenitor system may have been a galaxy with an initial mass  $6 \times 10^8 M_\odot$ , whose current position and final fate are unknown. According to this simulation, the tidal stream may be approximately ~2.8 Gyr of age. Our results demonstrate that NGC 4013, previously considered a prototypical isolated disk galaxy in spite of having one of the most prominent H I warps detected thus far, may have in fact suffered a recent minor merger. This discovery highlights that undisturbed disks at high surface brightness levels in the optical but warped in H I maps may in fact reveal complex signatures of recent accretion events in deep photometric surveys.

*Key words:* galaxies: dwarf – galaxies: evolution – galaxies: halos – galaxies: individual (NGC 4013) – galaxies: interactions

*Online-only material:* color figures

### 1. INTRODUCTION

In the last decade, the study of the formation and evolution of the Milky Way (MW) has been revolutionized by the first generation of wide-field, digital imaging surveys. The resulting extensive photometric databases have revealed for the first time the existence of spectacular stellar tidal streams (e.g., that from the Sagittarius dwarf galaxy; Ibata et al. 2001; Martínez-Delgado et al. 2001; Majewski et al. 2003) as well as large stellar substructures in the halo (Newberg et al. 2002; Rocha-Pinto et al. 2004; Juric et al. 2008), interpreted as the fossils of the hierarchical formation of our Galaxy. The discovery of the Monoceros tidal stream (Newberg et al. 2002; Yanny et al. 2003), located close to the Galactic plane outside the MW disk (as well as similar structures seen around the M31 disk; Ibata et al. 2005), indicates that mergers might play a relevant role in the formation of the outer regions of spiral disks (Peñarrubia et al. 2006) like that of the MW. Moreover, inside-out disk formation from continual accretion of in-falling material is an observed feature in cold dark matter (ΛCDM) simulations of the growth of structures on galaxy-sized scales (e.g., Abadi et al. 2003), and is now also a common feature of galactic chemical evolution models (e.g., Alibés et al. 2001; Chiappini et al.

2001) attempting to explain trends in disk chemical abundance patterns. These various results provide clear evidence that the destruction of satellite galaxies plays a relevant role not only in the formation of MW-like spiral galaxies generally but also for their disks as well as their halos. Furthermore, these results suggest that the stellar mass assembly of the MW disk, and disks in general, likely continues actively to the present epoch.

The accretion of satellite galaxies on low-inclination orbits may be an important formation mechanism of galactic disks in the ΛCDM paradigm (e.g., Abadi et al. 2003). The existence of low-inclined tidal streams in the outer regions of our Galaxy (e.g., the Monoceros or Triangulum/Andromeda tidal streams; Yanny et al. 2003; Majewski et al. 2003; Grillmair 2006) supports this prediction, although the external origin of these overdensities is still a matter of debate, mainly due to the severe extinction hindering the exploration of low-latitude areas. Recently, for example, Kazantzidis et al. (2008) and Younger et al. (2008) have suggested that, in a ΛCDM context, the bombardment by dark matter subhalos of an initially cold disk formed at  $z \simeq 1$  would also yield the formation of low surface brightness substructures ( $\mu \lesssim 25$  mag arcsec<sup>-2</sup>) with filamentary shape that may locally resemble tidal streams in phase space. Clearly, additional observational data (e.g., detailed chemical abundances) obtained along the Monoceros stream are needed to distinguish between both theoretical scenarios.

The search for extragalactic analogies to MW minor mergers is required not only to (1) show that the MW is not unusual in this respect but also to (2) obtain externally viewed “snapshots”

<sup>8</sup> Ramón y Cajal Fellow.

<sup>9</sup> Present address: Department of Astronomy, Penn State University, 525 Davey Lab, University Park, PA 16802, USA.

<sup>10</sup> Visiting Astronomer, Kitt Peak National Observatory.

of different phases of such interactions, (3) explore the range of possible mass/orbit combinations for such activity, and (4) estimate the fractional contribution of accreted mass and the mass spectrum of such events in the life of MW-like systems, an issue that remains unresolved (Majewski 1999). In this way, a systematic survey of tidal streams around other, nearby disk galaxies can provide new constraints and insights on the hierarchical formation and structure of MW-like galaxies beyond the previously limited views afforded by our own Galaxy and M31 (Ibata et al. 2007). A need to build up statistical information on the number and distribution of tidal streams in galaxies is driven by the availability of state-of-the-art, high-resolution cosmological simulations that offer, for the first time, the opportunity to use these observations to probe the theoretical predictions of galaxy formation in the framework of the  $\Lambda$ CDM paradigm (e.g., Bullock & Johnston 2005).

Promising galaxies in the hunt for extragalactic tidal streams are those displaying outstanding asymmetries in optical or H I images. It has long been suggested that these perturbations are a result of gravitational interaction with nearby companions. In some cases, apparently isolated galaxies exhibit morphologies more commonly associated with interacting systems. Recently, the prototypical isolated, warped disk galaxy, NGC 5907, was found to be surrounded by a spectacular stellar tidal stream (Shang et al. 1998; Martínez-Delgado et al. 2008), but one with no obvious companion (which may have been completely disrupted). In the case of both the MW and M31, there are also obvious disk warps—both stellar and gaseous—but no immediately obvious perturber, though small, nearby, likely tidally disrupting companion satellites have been suggested as a cause in each case (Sato & Sawa 1986; Ibata & Razoumov 1998; Bailin 2003; Bailin & Steinmetz 2004). These examples suggest that spirals with warped disks but no large nearby companions, may have undergone *minor* mergers in the last gigayears.

Under this prepense, we have been observing disk galaxies to faint surface brightnesses in the search for evidence of minor mergers. We (Martínez-Delgado et al. 2008) have previously reported our observations of the debris of a minor merger around the NGC 5907 disk system. Here, we report similar work on the edge-on disk, NGC 4013. NGC 4013 is one of the 62 luminous ( $M_B < -16.9$ ) members of the Ursa Major cluster of galaxies, a nearby, late-type dominated, and low-mass galaxy cluster. According to the HYPERLEDA database, the mean heliocentric radial velocity of NGC 4013 ( $836 \text{ km s}^{-1}$ ) places it at a distance of 14.6 Mpc. It is also a relatively isolated system, with the two nearest, slightly more luminous, cluster neighbours (NGC 4051 and NGC 3938) at  $\sim 170/250$  kpc projected distance away. Classified as an Sb galaxy with a maximum observed rotational velocity of  $195 \text{ km s}^{-1}$  (Bottema 1996), an extinction-corrected total absolute magnitude of  $-20.1 M_{\text{abs } B\text{band}}$  (Verheijen & Sancisi 2001), an optical scale length of 2.8 kpc ( $40''$ ) (van der Kruit & Searle 1982) and an isophote 25 mag arcsec $^{-2}$  radius of 5.2 (de Vaucouleurs et al. 1991), NGC 4013 is very similar to the Milky Way. NGC 4013 is, moreover, famous for its prodigiously warped H I disk, with a line of nodes close to parallel with that of the line of sight and with one of the largest warp angles observed ( $\sim 25^\circ$ ). On one side, the warp extends out to about 8 kpc ( $2'$ ) from the nominal plane (Bottema et al. 1987; Bottema 1995, 1996). The box/peanut-shaped bulge of NGC 4013 with its “X”-like morphology indicates the presence of a bar being observed edge-on (Patsis & Xilouris 2006).

Here, we report the optical detection of a faint, low surface brightness, looplike structure that appears to be part of a giant,

low-inclination stellar tidal stream of a disrupted dwarf satellite looking very similar to the expected form of the Monoceros tidal stream. This looping structure suggests the likelihood of there having been a previous interaction of NGC 4013 with a low-mass companion. The fact that NGC 4013’s very prominently warped H I layer matches in shape and orientation those of the apparent tidal loop makes this galaxy system a very compelling example of the likely link between disk warps and mergers, and an interesting case study for models of warp formation.

## 2. OBSERVATIONS AND DATA REDUCTION

We observed NGC 4013 with three different telescopes and instruments. In each case, the same structures appeared, albeit with different degrees of clarity.

### 2.1. KPNO 0.9 m Telescope

NGC 4013 was initially observed with the Kitt Peak National Observatory (KPNO; now Wisconsin Indiana Yale and NAO, WIYN) 0.9 m,  $f/8$  telescope as part of a pilot survey of low surface brightness features (like stellar tidal streams) around warped, nearby disk galaxies by C.P. and S.R.M. The initial sample included NGC 3044, NGC 3079, NGC 3432, and NGC 4013, all edge-on systems of large angular size with H I warps but no nearby, massive companions (though, in the cases of NGC 3432 and NGC 3079, some associated or nearby low surface brightness or dwarf satellites). These disk systems resemble NGC 5907, which at the time of this pilot survey had already been shown to have a tidal loop by Shang et al. (1998), and, in the case of NGC 3044, a minor merger was already hypothesized (Lee & Irwin 1997).

The observations were made with the Mosaic camera during several nights (UT 2000 March 31 to 2000 April 4) using the BATC 9 filter—essentially a narrow version of the Cousins  $R$  band—used by Shang et al. (1998) in their imaging of NGC 5907; the filter was kindly loaned by Rogier Windhorst. The Mosaic camera is made of eight  $2\text{k} \times 2\text{k}$  individual chips and provides a field of view (FOV) of  $59'$  at a pixel scale of  $0''.43 \text{ pixel}^{-1}$ . The conditions for this KPNO run were photometric, with a typical seeing of  $\sim 1''.3$ . Using standard IRAF procedures for the overscan/bias correction and flat-fielding, we combined the final image (see the upper panel of Figure 1) of NGC 4013 from the sum of four 1200 s exposures, eight 1800 s exposures, and one 900 s exposure.

A very faint arc is clearly identified in this image, situated at  $\sim 6'$  northeast of the center of the galaxy in the region of the extreme of northern plume of the gaseous warp (Bottema 1996; see Section 4). However, as may be seen, the achievable flat-fielding and surface brightness limit was not adequate to make definitive conclusions about the nature of this structure.

### 2.2. Isaac Newton Telescope

To confirm and better trace the extent of this structure, follow-up observations were obtained with the 2.5 m Isaac Newton Telescope (INT) at La Palma using the Wide Field Camera (WFC) at  $f/3.29$ . This instrument holds four  $4096' \times 2048'$  pixels EEV CCDs with a pixel size of  $0''.332$ , providing a total field of about  $35' \times 35'$ . Images were acquired during two service nights (UT 2003 March 27 and 2003 April 3) using the Sloan  $r'$  (#214) and Harris  $B$  (#191) filters. From the first night, we have two 600 s  $r'$ -band exposures, and from the second night three additional 600 s  $r'$ -band images plus four 1350 s  $B$ -band exposures.

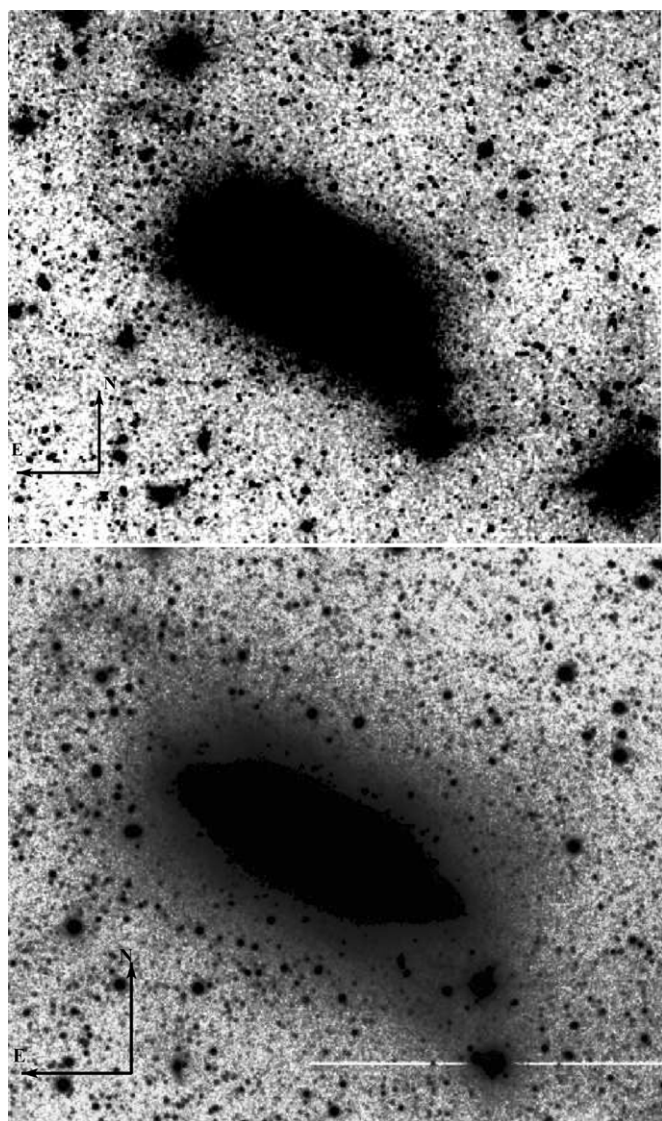


**Figure 1.** NGC 4013: smoothed and enhanced versions of KPNO 0.9 m image (upper panel) and INT  $B$ -band image (lower panel) highlighting low surface brightness features. The arrows of lengths  $2'$  in the lower left corner give the size and orientation. Both images are displayed in logarithm scale.

The central CCD (chip 4) was large enough (FOV  $22\frac{7}{8} \times 11\frac{1}{4}$ ) to include NGC 4013 and its warp, so we reduced only chip 4 in isolation, using standard IRAF procedures for the overscan/bias correction, flat-fielding, and combining of the individual images. The background on the final  $B$ -band image turned out to be flat and we obtained a sky value of  $22.22$  B-mag arcsec $^{-2}$  from ellipse fits, using the fixed outer disk geometry, beyond the galaxy as described in Pohlen & Trujillo (2006). The resulting  $3\sigma$  uncertainty on the sky value is below 0.04%. However, the individual  $R$ -band exposures suffered from scattered light causing large-scale variations in the background of the order of 2%. After careful masking of all sources, which were replaced by the mean of a linear interpolation along lines and columns, we used the IRAF *imsurf* routine on a median filtered ( $\sim 30''$  window) version of the masked and interpolated image to determine the background on each individual one. After subtracting this second-order fit from the images, they were combined to the final  $r'$ -band version reducing the large-scale variations in the background to 0.2%. The two images used in

**Table 1**  
Journal of Observations (Black Bird Observatory)

Date	Filter	$N_f$	Exp. Time (s)	Total Exp. Time (s)
2006 Nov 20	CL	8	900	7200
2006 Dec 17	CL	7	1800	12600
2006 Dec 24	Red	2	900	1800
2006 Dec 24	Green	1	540	540
2006 Dec 24	Blue	1	1080	1080
2006 Dec 27	CL	8	1800	14400
2006 Dec 28	Red	4	900	3600
2006 Dec 28	Green	5	540	2700
2006 Dec 28	Blue	5	1080	5400

this study have an equivalent exposure time of 50 minutes for the  $r'$  band and 90 minutes for the  $B$  band. Due to the unstable weather conditions (high humidity, sometimes cirrus) during the two nights, we did not use the observed standard stars, but obtained our photometric calibration from the  $r'$  and  $g'$  band Sloan Digital Sky Survey (SDSS; York et al. 2000) by means of aperture photometry. After geometrically mapping the two INT and two SDSS images to the same scale and center and applying an identically sized, but conservative (i.e., large) mask on the disturbing, bright star close to the center of NGC 4013, we obtained fluxes in six concentric apertures ( $40''$ – $240''$  diameter) on all four images. Following Smith et al. (2002), we converted the magnitudes measured on the SDSS images to Cousins  $R$  and Johnson  $B$ , and obtained the photometric zero points for our INT images using a linear fit without a color term. The uncertainty is of the order of 0.01 mag. We get similar results by using aperture photometry of six isolated, bright, but unsaturated stars. All the following magnitudes are given in  $R$  and  $B$ , correcting for Galactic extinction, ( $A_B = 0.072$ ,  $A_R = 0.044$ ; Schlegel et al. 1998), but not for inclination.

The final image of NGC 4013 is shown in the lower panel of Figure 1. Although the background is still an issue, we can now more confidently trace and measure the low surface brightness arc. It is important to remark that all quoted surface brightness measurements in this paper (see Section 3) come from the data set obtained at this telescope, the only one where we have calibrated, deep-enough photometric data.

### 2.3. Black Bird Remote Observatory Telescope

The evidence of a possible tidal stream around NGC 4013 from our previous data obtained with the KPNO telescope and INT motivates us to select this galaxy as a priority target in our pilot survey of stellar tidal streams in nearby spiral galaxies using small telescopes, of which searching strategy was successfully proven with the detection of very faint parts of the NGC 5907 tidal stream (the commissioning target of this survey; see Martínez-Delgado et al. 2008).

With this purpose, we obtained very deep images of NGC4013 with the  $f/8.3$  Ritchey–Chrétien 0.5 m telescope of the Black Bird Remote Observatory (BBRO) situated in the Sacramento Mountains (NM, USA). The data was obtained during several dark sky observing runs between UT 2006 November 6 and UT 2006 December 28. We used a Santa Barbara Instrument Group (SBIG) STL-11000 CCD camera, which yields a large field of view ( $27\frac{7}{8} \times 18\frac{1}{2}$ ) and a plate scale of  $0\prime.45$  pixel $^{-1}$ . The data consists of multiple deep exposures through noninfrared clear luminance (CL;  $3500 < \lambda < 8500$ ), red, green, and blue filters from the SBIG Custom Scientific filters set. Table 1 gives a summary of the images collected for this project.

Column 5 refers to the total exposure time of the coadded images for each filter obtained with each run. This yields a total exposure time per filter of 5400 s (red), 3240 s (green), 6480 s (blue), and 39600 s (CL).

A master dark and bias frame was created by combining 10 dark subexposures each produced at the same exposure length and camera temperature settings used for the luminance and the filtered exposures. A master flat was produced by combining 10 separate sky flat exposures for each filter. The science data subexposures were reduced using standard procedures for bias correction and flat fielding. The data captured through the CL filter was median-combined to produce a master CL-filter data set. The red, green, and blue filtered exposures were separately combined (using the median technique) to produce individual red, green, and blue master images that represented the total exposure time through each color filter. The resulting data sets for each color filter were subsequently summed to produce a “synthetic” luminance image that represented the total exposure time accumulated through all of the color filters, which was subsequently summed and combined with the CL-filter image. The resulting final image thus represented the sum of all available CCD exposures collected in this project, with an accumulated exposure time of 15.2 hr (including 11 hr through a clear luminance filter).

The dynamic range of the final image was very large, because of the presence of a very bright, galactic disk surrounded by very diffuse tidal stream. To optimize the contrast of the faint structures detected around NGC 4013, we used a histogram equalization of the image by means of a nonlinear transfer function.<sup>11</sup> This well-known image processing technique employs a monotonic, nonlinear mapping that reassigns the intensity values of pixels in the input image such that the output image contains a uniform distribution of intensities. This yields an effective method to suppress the bright regions of the image, intensifying the fainter parts of the stream. In addition, to increase the signal-to-noise of the faint structures surrounding NGC 4013, image noise effects were reduced by the application of a Gaussian filter (Davies 1990). An illustrative example of the effect of these processes is given in Figure 2.

The final image of NGC 4013 was obtained using an iterative process that involves several passes of an S-shaped histogram operator to the total image and the application of a 3 pixel diameter low-pass Gaussian filter. This approach optimized contrast and detail throughout the tonal range of the image and permitted the faint structure surrounding NGC 4013 to be rendered distinguishable in the final image. The resulting image is shown in Figure 3. We have added the labels A through G to identify some photometric feature that we discuss in the following section.

As discussed in Martínez-Delgado et al. (2008), the search strategy of this survey was designed to obtain the position and morphology of very faint structures around the spiral galaxy, with the aim of providing a guide for pencil-beam, follow-up photometric surveys in state-of-art telescopes. Because this approach is mainly based on the use of a very broadband, uncalibrated luminance filter, the BBRO telescope data is only used in this paper to discuss the overall morphology of the possible stream. From our previous experience (e.g., NGC 5907: Martínez-Delgado et al. 2008; Messier 94: I. Trujillo et al. 2009, in preparation), we estimate that the final image should include diffuse light structures as faint as  $\mu_R \sim 29$  mag arcsec<sup>-2</sup>.

<sup>11</sup> See <http://homepages.inf.ed.ac.uk/rbf/HIPR2/histeq.htm> and references within.

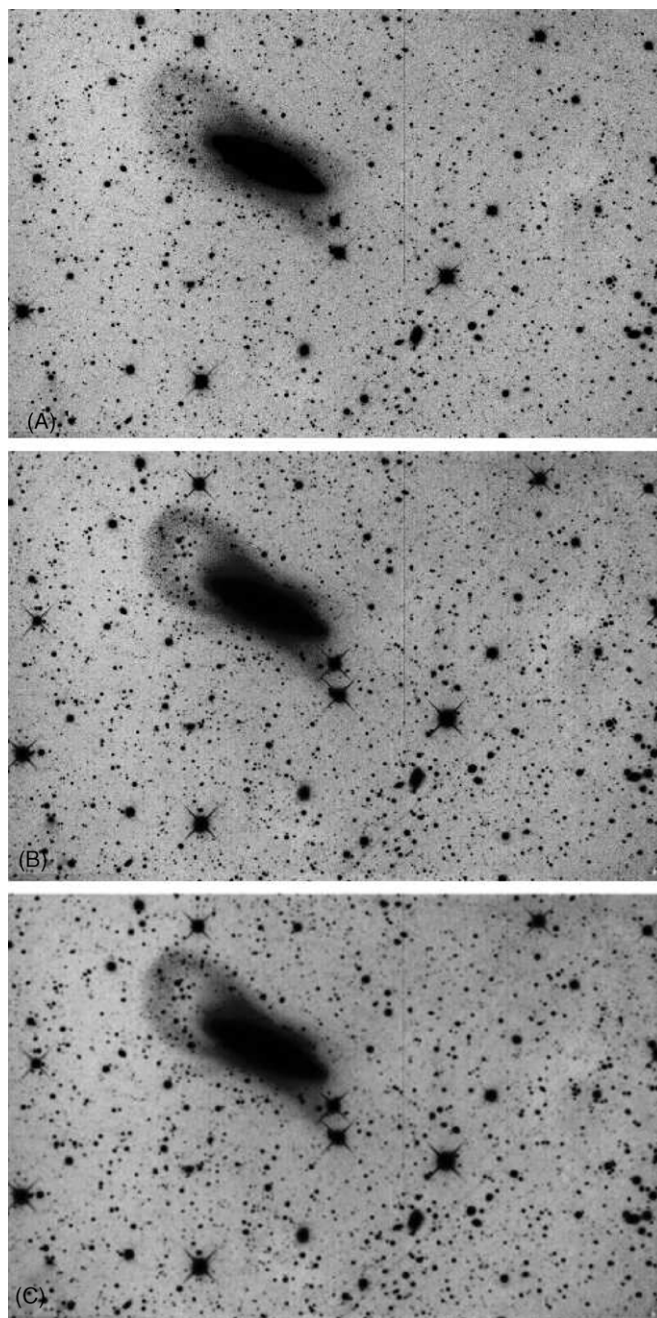


**Figure 2.** An illustrative example of the effect of histogram equalization and Gaussian filtering techniques in the resulting final image obtained from the sum of all the exposures taken with the BBRO: (A) the image with linear stretching (and thus nonprocessed); (B) the image after applying an histogram equalization with a nonlinear function; and (C) the effect of a Gaussian filter of 5 pixels of radius in the summed image displayed in panel A. The blurrier aspect of this image with respect to the final version displayed in Figure 3 is due the larger filter width used here to enhance the effect of the filter with illustrative purposes. The field of view of these images is  $28' \times 18'$ .

### 3. THE TIDAL STREAM(S) OF NGC 4013

In addition to the well known peanut-shaped bulge (van der Kruit & Searle 1982; feature A in Figure 3) with a full vertical extent of about 2 kpc ( $30''$ ), a contour plot of the INT image (Figure 4) reveals a huge, at least 13 kpc ( $> 3'$ ) sized box-shaped outer “stellar halo” (feature B in Figure 3 and also obvious in the images in Figure 1). Furthermore, to the east, a striking horseshoe-like structure (feature C in Figure 5) is visible in the

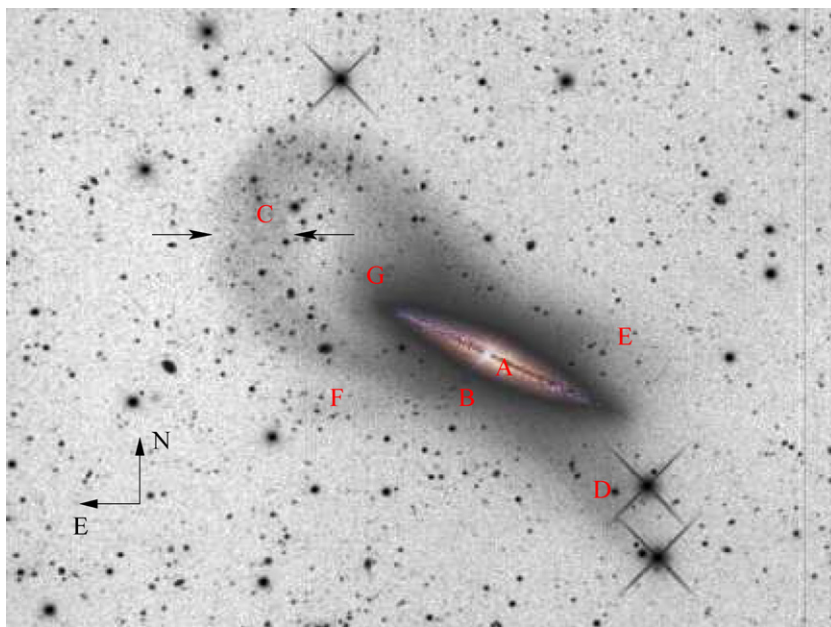


**Figure 3.** Image of NGC4013 obtained with the BBRO 20 inch telescope. The total exposure time of the original image was 13.7 hr (including 11 hr in luminance clear-filter) and was noise-filtered by applying a Gaussian filter. The image has dimensions of  $\sim 16.8 \times 12.8$ , which, at the distance of NGC 4013 is  $\sim 71 \times 54$  kpc. Identified photometric features labeled A–G are discussed in Section 3. For illustrative purpose, a color image of the NGC 4013 obtained with the same telescope has been superimposed on the saturated disk region of the galaxy.

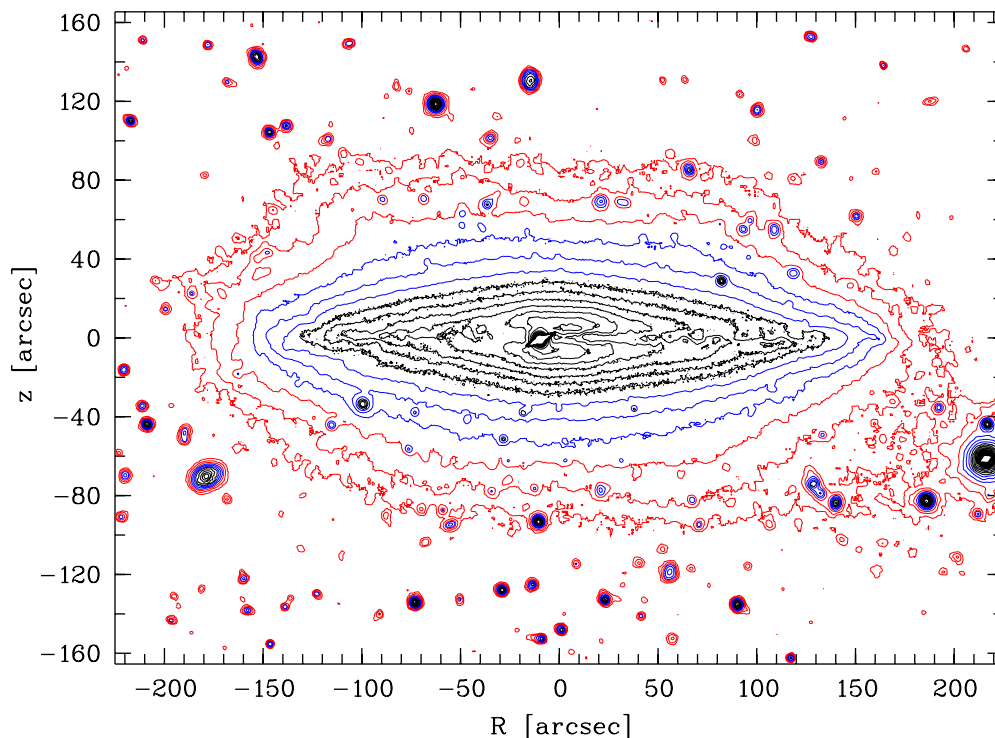


**Figure 4.** Isaac Newton Telescope *B*-band contour map of NGC 4013 highlighting the box-shaped outer halo. Contours are at levels 17.0–27.0 *B*-mag arcsec<sup>-2</sup> in equidistant steps of 0.5 mag. Toward the outer parts, we smoothed the contours using three increasing levels of median filtering (indicated by the three different colors).

BBRO image, starting at the northeast corner of the box-shaped halo and reaching out to at least 26 kpc ( $6'$ ) from the center. This feature, that corresponds to the arc detected in the KPNO and INT images (see Section 2 and Figure 1), is now evident as looplike. The obvious hole in the light distribution clearly shows that this feature is not simply a stellar warp, but an actual “ringlike” structure seen obliquely, and of the type produced by tidal streams (see Section 4). The loop apparently enters the

galaxy again at the southeast corner of the box (labeled F in Figure 3).

The BBRO and INT images also show a pair of *wings* jutting to the west and southwest (features D and E) and straddling this side of the NGC 4013 disk, *squaring off* the most diffuse galaxy light distribution at large radii. In the diffuse light visible in the northwest edge of the galaxy (feature E), there is some evidence for a shorter, coherent loop feature visible in a

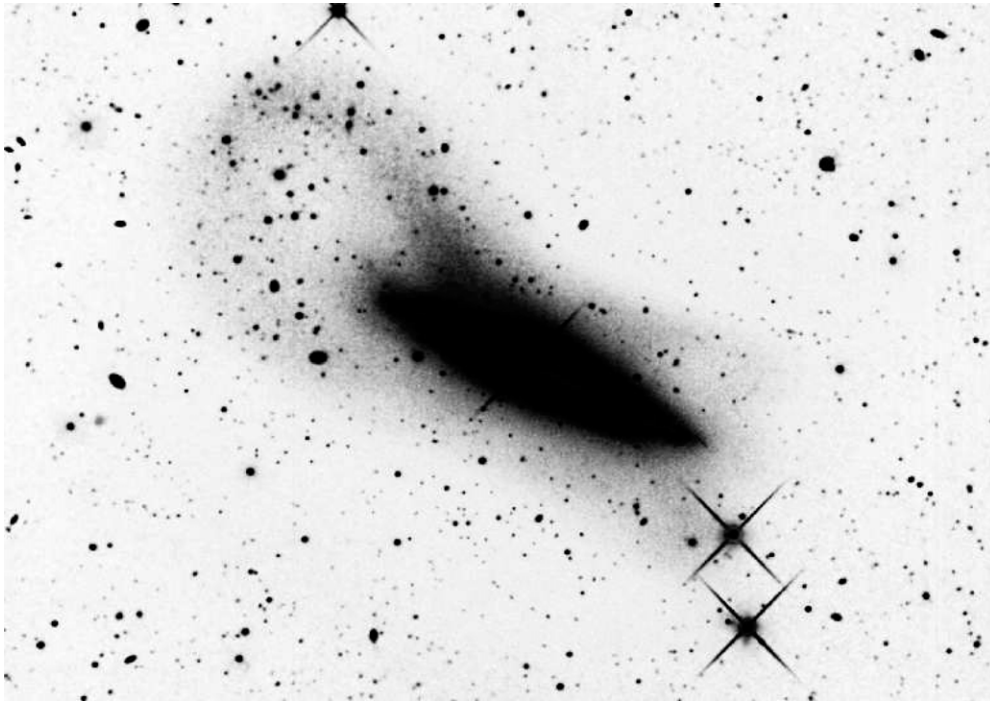


**Figure 5.** High-stretched version of the luminance clear-filter image of NGC 4013 obtained with the BBRO telescope. This shows evidence of a possible second arm of debris within the diffuse light wind to the northwest edge of the NGC4013 disk (feature E in Figure 3). In addition, the spikelike feature visible in the northeast edge of the disk could be related to the stellar component of the prodigious gaseous warp of the galaxy. North is up and east to the left.

high-contrasted version of the BBRO image (Figure 5). This is consistent with the presence of a second arm of debris (as expected in theoretical simulations, see Section 4), which is probably related to the northeast loop (feature C). However, deeper images are necessary to confirm this hypothesis. The more plumelike feature visible on the southwest side (feature D in Figure 3) extends  $\sim 17$  kpc ( $4'$ ) out. Unfortunately, the clarity of this feature (also barely visible in the INT image in Figure 1) is somewhat hindered by the presence of two bright stars.

Together, these wings, and the obvious loop to the northeast could be seen as parts of one continuous *ribbon-bow* or *pretzel-like* structure surrounding the disk but with arms that cross each other at the galaxy center (at least in projection). Evidently, these particular features of the extended light distribution are the result of a single, coherent tidal disruption event, which is creating a low-inclination stellar stream around the disk of NGC 4013. An example of how such a tidal structure might be formed is shown in a tidal disruption model (see Figure 6 and Section 4). It is worth noting that we do not observe any bright spot that could be identified with a remaining, intact dwarf galaxy core among any of the low surface brightness features. Therefore, our images do not provide any evidence on the final fate of the progenitor galaxy, which could be hidden inside the disk or could be completely disrupted by now.

The surface brightness of the described structures is very close to the remaining inhomogeneities in the background of our CCD INT images, specially on the  $r'$ -band image, which makes it extremely difficult to determine accurate surface brightnesses. Using a set of small  $\approx 4'' \times 4''$  boxes, strategically placed along the stream by avoiding stars and any residual obvious brightness condensation, we estimated the mean surface brightness of the stream on the east side (feature C) to be about  $\mu_B = 28.6^{+0.6}_{-0.4}$  and  $\mu_R = 27.0^{+0.3}_{-0.2}$ . The large errors are due to the uncertainty of  $\sim 0.1\%$  in the local sky determination (a set of similar small boxes placed outside, but close to the stream) and are

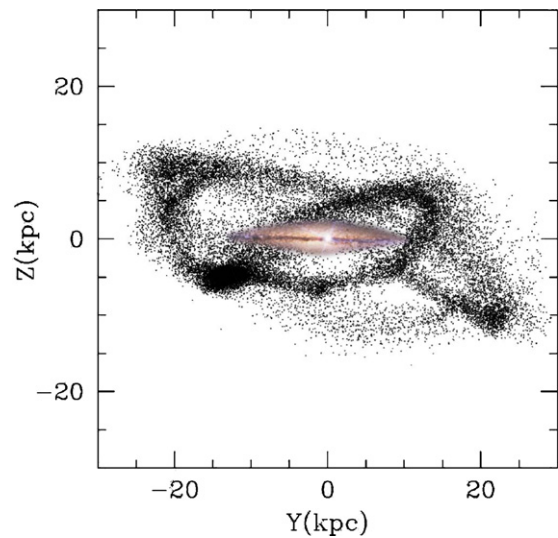


**Figure 6.**  $X$ - $Y$  galaxy plane projection of the prograde model *pro1* of the Monoceros tidal stream by Peñarrubia et al. (2005). For comparison purposes, a color image of the NGC 4013 disk (see Figure 3) has been scaled (assuming a distance of 14.6 Mpc) and superimposed to the distribution of debris. The comparison of this model snapshot to the structures detected in NGC 4013 provides considerable support for the hypothesis that they consist of different pieces from a single tidal stream. The NGC 4013 disk (and the residual light of its box-shaped outer halo shown in Figure 5, not simulated here) almost overlaps the full path of the stream that emerges as individual looplike structures of debris (or winds) at large galactocentric radius (features C and E in Figures 3 and 5). (A color version of this figure is available in the online journal.)

of the same order as the brightness variation along the stream. This yields a  $(B-R)$  color of  $1.6^{+0.6}_{-0.4}$ , which is a typically red value found for S0 galaxies (e.g., Barway et al. 2005), and would be consistent with the redder dwarfs of the Local Group (Mateo 1998). Although the color of the loop is about 0.6 mag

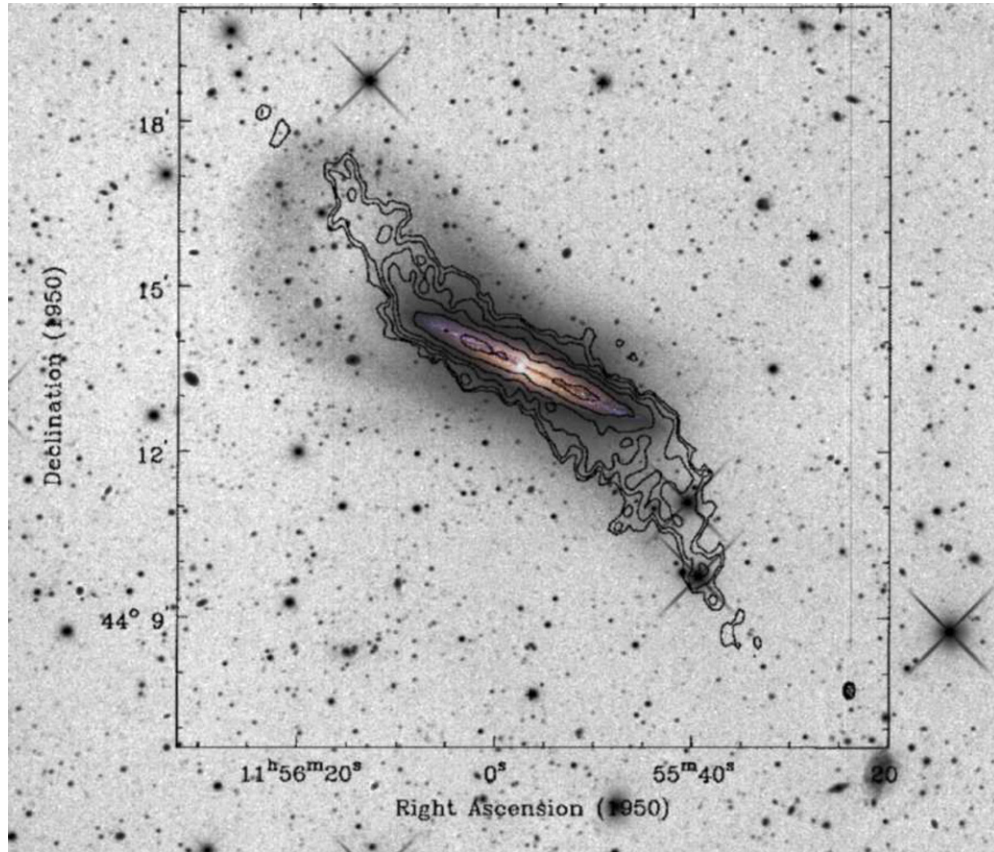


**Figure 7.** Overlay of the H I contours from Bottema (1996; his Figure 1) on our BBO image of NGC 4013. The lowest H I contour level shown is about  $1 \times 10^{20}$  H atoms  $\text{cm}^{-1}$ . The beam is given in the lower right corner of the H I insert. The scale of this image is  $\sim 4.2$  kpc  $\text{arcmin}^{-1}$ .

(A color version of this figure is available in the online journal.)

redder than the outer (radially/vertically) parts of the disk/halo of NGC 4013 and only close to the midplane of the galaxy (where the dust lane certainly reddens the intrinsic colors), we find similar colors as for the stream within the attached large error. Therefore, deeper broadband observations are needed to undoubtedly conclude whether its stellar population is not composed of the same mix of stars found in the outer region of NGC 4013's disk, an additional evidence that this horseshoe-like feature did not originate in the disk itself.

The width of this giant stream is variable along its path, but this may be due to a projection effect. A rough estimate for the full width at half-maximum (FWHM) of the stream  $1.0 \pm 0.3$  kpc ( $\sim 14''$ ) is taken at the most distant part on the northeast side of feature C in Figure 3.

Figure 7 shows the position of the possible tidal stream with respect to the prominent H I gas warp (Bottema et al. 1987; Bottema 1996). This comparison clearly shows that there is no H I gas associated with the detected giant stellar feature (such as is the case in NGC 3310; Wehner & Gallagher 2005) on the northeast side (feature C). On this side, the projected path of the stream shows a very similar inclination to the warped gas disk, but is clearly outside and almost enclosing (in projection) the measured H I gas.

Interestingly, our high-contrasted version of the BBRO image (Figure 5) reveals the trace of a spikelike feature in the northeast edge of the galaxy disk (feature G), with a position and orientation with respect to the galactic plane that is consistent with the stellar counterpart of the prodigious gaseous warp. It is clear, however, that (at our surface brightness limit) this stellar component warp is significantly less extended than the

H I-component displayed in Figure 7. On the southeast side, the extended optical feature D (see Figure 3) seems to be associated to the southern H I gas plume of the warp, although on this side we are severely hampered by the two bright foreground stars. However, the clear separation of the H I gas and the optical light on the other side of the galaxy let us reject the direct association of these structures as an extended, low-luminosity stellar counterpart of the warped H I disk of NGC 4013.

#### 4. DISCUSSION

Our deep images of NGC 4013 show a complex stellar halo, including a coherent, streamlike structure inclined at  $\sim 25^\circ$  with respect to the galaxy disk. We have independently confirmed the presence of these low surface brightness features with three data sets from three different telescopes. In addition, if one knows what to look for, the loop is also barely visible on the Digitized Sky Survey 2 (DSS2) blue plate and on the archival  $4.5 \mu\text{m}$  *Spitzer* Infrared Telescope Facility image. The existence of the loop structure is therefore without question. The discovered structures are evidently debris material produced by the tidal disruption of a low-mass galaxy companion to NGC 4013. Such features are expected from tidal disruption of a companion galaxy (Johnston et al. 2001) and similar features are also observed in NGC 5907 (Shang et al. 1998; Martínez-Delgado et al. 2008), NGC 3310 (Wehner & Gallagher 2005), and a handful of other external galaxies (summarized in Table 1 in Martínez-Delgado et al. 2008).

The sky-projected geometry of this structure is in fact similar to the edge-on, external perspective of a tidal stream that results from the tidal disruption of a single dwarf galaxy satellite moving on a low-inclined orbit predicted by different theoretical simulations (e.g., the Monoceros tidal stream: Peñarrubia et al. 2005; Canis Major overdensity: Martin et al. 2004, their Figure 14). For comparison purpose, we will use here as template the  $N$ -body model constructed by Peñarrubia et al. (2005) to reproduce the geometry and kinematics of the Monoceros tidal stream. This model simulates the accretion of a low-mass satellite ( $6 \times 10^8 M_{\odot}$ ) on a nearly circular ( $e = 0.10 \pm 0.05$ ), low-inclined ( $i \sim 25^{\circ}$ ) orbit in the last 3 Gyr and provides a remarkable good match to the projected, edge-on view of the stream wrapping NGC 4013 (see Figure 6). Considering that NGC 4013 has a smaller disk scale length,  $h_R = 2.8$  kpc, and a lower maximum circular velocity,  $V_{c,\max} = 195 \text{ km s}^{-1}$  (Bottema 1996) than the Milky Way, we can apply dynamical considerations to estimate the stream age from the  $N$ -body model, so that  $\text{Age}/\text{Age}_{\text{Mon}} = h_R/h_{R,\text{MW}} \times V_{c,\max}/V_{c,\max,\text{MW}}$ . For the Milky Way we have that  $h_R = 3.5$  kpc and  $V_{c,\max} = 220 \text{ km s}^{-1}$ , thus  $\text{Age}/\text{Age}_{\text{Mon}} \approx 0.9$ . Since some pieces of the Monoceros stream are  $\text{Age}_{\text{Mon}} = 3$  Gyr old, we estimate that the stream surrounding NGC 4013 may be as old as  $\approx 2.8$  Gyr. However, although the model provides a reasonable qualitative resemblance to the morphology of NGC 4013, it cannot fully explain the observed structure. For example, while the observed tidal structure in Figure 3 is clearly more prominent on its eastern side of the galaxy, the model shows loops of roughly equal brightness on both sides (as well as various other features that not detected in our deep image). Unfortunately, with no kinematic data and only the projected geometry of the stream as constraint, the orbit and mass of the progenitor system may be degenerated, and in that respect the estimates presented here must be considered illustrative only.

Although the progenitor system of the Monoceros and NGC 4013 tidal streams might have shared similar orbits and initial masses, our estimates reveal that the surface brightness of the latter is approximately two to three magnitudes higher than the value reported for this low galactic latitude tidal debris candidate ( $\mu_B \sim 30.0 \text{ mag arcsec}^{-2}$ ; J. de Jong 2008, private communication). A possible explanation might be that the progenitor of the NGC 4013 stream was more luminous than that of the Monoceros stream. Since both models have the same initial mass, this hypothesis would imply that the mass-to-light ratio of the NGC 4013 stream progenitor was considerably lower than that of the Monoceros stream. However, the  $N$ -body models used by Peñarrubia et al. (2005) assume that the stellar and dark matter components of the progenitor system have the same spatial distribution (i.e., mass-follows-light models). In a  $\Lambda$ CDM cosmogony, stars only populate the innermost regions of dwarf galaxies (Strigari et al. 2007; Peñarrubia et al. 2008a) and can only be tidally stripped after most of the dark matter halo beyond the luminous radius has been lost (Peñarrubia et al. 2008b), which introduces an additional parameter: the spatial segregation of the stellar component with respect to the surrounding dark matter halo of the progenitor galaxy, which is fundamental to determine the survival time of dwarf galaxies and the properties of their associated tidal streams. For example, the more deeply embedded within the halo a stellar component is, the thinner, brighter, and colder will be its associated tidal stream. Therefore, for  $\Lambda$ CDM-motivated models, the halo size, the stellar spatial segregation, and the total luminosity of a dwarf galaxy are all parameters that influence the resulting surface

brightness of an associated tidal stream but which, unfortunately, cannot be constrained in the absence of additional data (e.g., kinematics).

Whereas the detection of the stream around NGC 4013 cannot shed light on the nature of the Milky Way stellar overdensities (including on the controversial origin of the Monoceros stream; see Section 1), it does suggest that the accretion of satellite galaxies on low-inclination, low-eccentric orbit may be relatively common during the hierarchical formation of spiral galaxies. In fact, their occurrence in the known sample of stellar tidal streams in the Local Volume ( $D < 15$  Mpc; see Martínez-Delgado et al. 2008; Pohlen et al. 2004) is  $\gtrsim 20\%$ . In this context, the presence of giant disks around spiral galaxies that extend out to several scale lengths of the inner disk (e.g., the extended disk found by Ibata et al. 2005 around M31 is detectable out to a projected radius of 80 kpc with the present instrumentation) might also be signature of the accretion of massive satellite galaxies moving on low-inclination, low-eccentricity orbits (Peñarrubia et al. 2006), adding support to the scenario that the disks of spiral galaxies may grow inside out as a result of this type of accretion events.

The detection of galactic warps in spiral galaxies that present signatures of recent accretion events is quickly increasing with the availability of wide-field, deep photometric surveys. Although the origin of galactic warps is still unknown, it was earlier proposed that the gravitational perturbations induced by satellite galaxies may cause the formation of warps (Burke 1957; although see Hunter & Toomre 1969 for counterarguments). Since those early studies, several alternative scenarios have been proposed in the literature. For example, it has been shown that the interaction of a stellar disk with the surrounding dark matter halo may also induce the formation of warps (Sparke & Casertano 1988; Binney et al. 1998), as well as bending instabilities (Revaz & Pfenniger 2004), intergalactic accretion flows onto the disk (López-Corredoira et al. 2002) and cosmic in-fall (Shen & Sellwood 2006).

A crucial fact that has been often invoked to dismiss the tidal origin of galactic warps was the existence of warped spiral galaxies in apparent isolation (Sancisi 1976). NGC 4013, with its prominent, and rather symmetrical H I warp, along with a really unassailable indication of a past merger event, provides an important counterexample to the above argument; indeed, NGC 4013 may well be the Rosetta Stone for warp theories, since morphologically the warp and the merger debris seem so closely aligned.

With NGC 5907 and NGC 4013, we have now two examples of apparently isolated galaxies with significantly warped gaseous disks, which at the same time show evidence for an ongoing tidal disruption of a dwarf companion. The connection between the warp of the MW and its satellite galaxies has already been explored in some recent studies. For example, Bailin (2003) and Weinberg & Blitz (2006) study the effects of the Sagittarius dwarf and the Magellanic Clouds on the MW disk, respectively. Interestingly, the existence of warped galaxies that have suffered a recent accretion of satellite galaxies on low-inclination, low-eccentricity orbits (like the MW and NGC 4013) suggests that these kind of accretion events may induce the formation of warps more efficiently than the perturbations from satellite galaxies moving on highly eccentric, nearly polar orbits. This is a possibility worth of investigation.

With the growing number of examples showing a connection between warped disks and evidence of mergers, even for disk systems with no obvious companions, we may be close to



resolving the mystery of warps, and in a way be consistent with prevailing  $\Lambda$ CDM models of galaxy formation.

We thank R. Bottema for making the H I contour map available to us. D.M-D acknowledges funding from the Spanish Ministry of Education (Ramon y Cajal program contract and research project AYA 2004-08260-C03-02). C.P. and S.R.M. thank R. Windhorst for the loan of the BATC 9 filter for the KPNO 0.9-m observations. Part of this work was supported by a Marie Curie Intra-European Fellowship within the 6th European Community Framework Programme. C.P. and S.R.M. thank R. Windhorst for the loan of the BATC 9 filter for the KPNO 0.9-m observations. S.R.M. acknowledges support from the National Science Foundation grants AST 97-02521 and AST 03-07851, a Cottrell Scholar Award from the Research Corporation, NASA/JPL contract 1228235, the David and Lucile Packard Foundation, and the generous support of The F. H. Levinson Fund of the Peninsula Community Foundation. J.P. thanks J. F. Navarro for financial support. Funding for the creation and distribution of the SDSS Archive has been provided by the Alfred P. Sloan Foundation, the Participating Institutions, the National Aeronautics and Space Administration, the National Science Foundation, the U.S. Department of Energy, the Japanese Monbukagakusho, and the Max Planck Society. The SDSS Web site is <http://www.sdss.org/>. This research has made use of the Online Digitized Sky Surveys (DSS1 & 2) server at the ESO/ST-ECF Archive produced by the Space Telescope Science Institute through its Guide Star Survey group.

## REFERENCES

- Abadi, M. G., Navarro, J. F., Steinmetz, M., & Eke, V. R. 2003, *ApJ*, **597**, 21
- Alibés, A., Labay, J., & Canal, R. 2001, *A&A*, **370**, 1103
- Bailin, J. 2003, *ApJ*, **583**, L79
- Bailin, J., & Steinmetz, M. 2004, in *Satellites and Tidal Streams*, ed. D. Martínez-Delgado, F. Prada, & T. J. Mahoney (San Francisco, CA: ASP), 225
- Barway, S., Mayya, Y. D., Kembhavi, A. K., & Pandey, S. K. 2005, *AJ*, **129**, 630
- Binney, J., Jiang, I.-G., & Dutta, S. 1998, *MNRAS*, **297**, 1237
- Bottema, R. 1995, *A&A*, **295**, 605
- Bottema, R. 1996, *A&A*, **306**, 345
- Bottema, R., Shostak, G. S., & van der Kruit, P. C. 1987, *Nature*, **328**, 401
- Bullock, J. S., & Johnston, K. V. 2005, *ApJ*, **635**, 931
- Burke, B. F. 1957, *AJ*, **62**, 90
- Chiappini, C., Matteucci, F., & Romano, D. 2001, *ApJ*, **554**, 1044
- Davies, E. 1990, *Machine Vision: Theory, Algorithms and Practicalities* (New York: Academic), 42
- de Vaucouleurs, G., de Vaucouleurs, A., Corwin, H. G., Buta, R. J., Paturel, G., & Fouque, J. B. 1991, *Third Reference Catalogue of Bright Galaxies* (New York: Springer)
- Grillmair, C. 2006, *ApJ*, **651**, 29
- Hunter, C., & Toomre, A. 1969, *ApJ*, **155**, 747
- Ibata, R., Chapman, S., Ferguson, A. M. N., Lewis, G., Irwin, M., & Tanvir, N. 2005, *ApJ*, **634**, 287
- Ibata, R., Irwin, M., Lewis, G., Ferguson, A. M. N., & Tanvir, N. 2001, *Nature*, **412**, 49
- Ibata, R., Irwin, M., Lewis, G. F., & Stolte, A. 2001, *ApJ*, **547**, L133
- Ibata, R., Martin, N. F., Irwin, M., Chapman, S., Ferguson, A. M. N., Lewis, G. F., & McConnachie, A. W. 2007, *ApJ*, **671**, 1591
- Ibata, R. A., & Razoumov, A. O. 1998, *A&A*, **336**, 130
- Johnston, K. V., Sackett, P. D., & Bullock, J. S. 2001, *ApJ*, **557**, 137
- Juric, M., et al. 2008, *ApJ*, **673**, 864
- Kazantzidis, S., Bullock, J. S., Zentner, A. R., Kravtsov, A. V., & Moustakas, L. A. 2008, *ApJ*, **688**, 254
- Lee, S.-W., & Irwin, J. A. 1997, *ApJ*, **490**, 247
- López-Corrodoira, M., Betancort-Rijo, J., & Beckman, J. E. 2002, *A&A*, **386**, 169
- Majewski, S. R. 1999, in *The Third Stromlo Symposium: The Galactic Halo*, ed. B. Gibson, T. Axelrod, & M. Putman (San Francisco, CA: ASP), 76
- Majewski, S. R., Ostheimer, J. C., Rocha-Pinto, H. J., Patterson, R. J., Guhathakurta, P., & Reitzel, D. 2004, *ApJ*, **615**, 738
- Majewski, S. R., Skrutskie, M. F., Weinberg, M. D., & Ostheimer, J. 2003, *ApJ*, **599**, 1082
- Martin, N. F., Ibata, R. A., Bellazzini, M., Irwin, M. J., Lewis, G. F., & Dehnen, W. 2004, *MNRAS*, **348**, 12
- Martínez-Delgado, D., Aparicio, A., Gómez-Flechoso, M. A., & Carrera, R. 2001, *ApJ*, **549**, L199
- Martínez-Delgado, D., Peñarrubia, J., Gabany, R. J., Trujillo, N., Majewski, S. R., & Pohlen, M. 2008, *ApJ*, **689**, 184
- Mateo, M. L. 1998, *ARA&A*, **36**, 435
- Newberg, H. J., et al. 2002, *ApJ*, **569**, 245
- Patsis, P. A., & Xilouris, E. M. 2006, *MNRAS*, **366**, 1121
- Peñarrubia, J., McConnachie, A., & Babul, A. 2006, *ApJ*, **650**, L33
- Peñarrubia, J., McConnachie, A. W., & Navarro, J. F. 2008a, *ApJ*, **672**, 904
- Peñarrubia, J., Navarro, J. F., & McConnachie, A. W. 2008b, *ApJ*, **673**, 226
- Peñarrubia, J., et al. 2005, *ApJ*, **626**, 128
- Pohlen, M., Martínez-Delgado, D., Majewski, S., Palma, C., Prada, F., & Balcells, M. 2004, in *Satellites and Tidal Streams*, ed. M.-D. Prada, T. J. Mahoney (San Francisco, CA: ASP), 288
- Pohlen, M., & Trujillo, I. 2006, *A&A*, **454**, 759
- Revaz, Y., & Pfenniger, D. 2004, *A&A*, **425**, 67
- Rocha-Pinto, H. J., Majewski, S. R., Skrutskie, M. F., Crane, J. D., & Patterson, R. J. 2004, *ApJ*, **615**, 732
- Sancisi, R. 1976, *A&A*, **53**, 159
- Sato, N. R., & Sawa, T. 1986, *PASJ*, **38**, 63
- Schlegel, D. J., Finkbeiner, D. P., & Davis, M. 1998, *ApJ*, **500**, 525
- Shang, Z., et al. 1998, *ApJ*, **504**, L23
- Shen, J., & Sellwood, J. A. 2006, *MNRAS*, **370**, 2
- Smith, J. A., et al. 2002, *AJ*, **123**, 2121
- Sparke, L. S., & Casertano, S. 1988, *MNRAS*, **234**, 873
- Strigari, L. E., Koushiappas, S. M., Bullock, J. S., & Kaplinghat, M. 2007, *Phys. Rev. D*, **75**, 083526
- van der Kruit, P. C., & Searle, L. 1982, *A&A*, **110**, 61
- Verheijen, M. A. W., & Sancisi, R. 2001, *A&A*, **370**, 765
- Wehner, E. H., & Gallagher, J. S., III. 2005, *ApJ*, **618**, L21
- Weinberg, M. D., & Blitz, L. 2006, *ApJ*, **641**, L33
- Yanny, B., et al. 2003, *ApJ*, **588**, 824
- York, D. G., et al. 2000, *AJ*, **120**, 1579
- Younger, J. D., Besla, G., Cox, T. J., Hernquist, L., Robertson, B., & Willman, B. 2008, *ApJ*, **676**, L21